BRDF profile of Tyvek and its implementation in the Geant4 simulation toolkit

Libor Nozka,* Miroslav Pech, Helena Hiklova, Dusan Mandat, Miroslav Hrabovsky, Petr Schovanek and Miroslav Palatka

Regional Centre of Advanced Technologies and Materials, Joint Laboratory of Optics, Faculty of Science, Palacky University, 17. Listopadu 50a, 771 46 Olomouc, Czech Republic

**libor.nozka@upol.cz*

Abstract: Diffuse and specular characteristics of the Tyvek 1025-BL material are reported with respect to their implementation in the Geant4 Monte Carlo simulation toolkit. This toolkit incorporates the UNIFIED model. Coefficients defined by the UNIFIED model were calculated from the bidirectional reflectance distribution function (BRDF) profiles measured with a scatterometer for several angles of incidence. Results were amended with profile measurements made by a profilometer.

OCIS codes: (120.5820) Scattering measurements; (240.6700) Surfaces; (290.1483) BSDF, BRDF, and BTDF.

References and links

1. C. Yanagisawa for the Super-Kamiokande Collaboration, "The Super-Kamiokande detector," Nucl. Instrum. Meth. A, **501**, 418462 (2003).
2. I. Allekotte for the Pierre Auger Collaboration, "The surface detector system of the Pierre Auger Observatory," Nucl. Instrum. Meth. A, **586**, 409-420 (2008).
3. J. Allison for Geant4 Collaboration, "Geant4 - A Simulation Toolkit," Nucl. Instrum. Meth. A, **506**, 250-303 (2003).
4. Geant4 Collaboration, "Geant4 Developments and Applications," IEEE T. Nucl. Sci., **53**, no. 1, 270-278 (2006).
5. G. Santin, D. Strul, D. Lazaro, L. Simon, M. Krieguer, M. Vieira Martins, V. Breton and C. Morel, "GATE: A Geant4-Based Simulation Platform for PET and SPECT Integrating Movement and Time Management," IEEE T. Nucl. Sci. **50**(5), 15161521 (2003).
6. A. Levin and C. Moisan, "A more physical approach to model the surface treatment of scintillation counters and its implementation in DETECT," Proc. IEEE Nucl. Sci. Symp., **2** (1996).
7. J. C. A. Velazquez, C. V. Lopez and A. Zepeda, "Diffuse reflectivity of Tyvek in air and water, and anisotropical effects," Nucl. Instrum. Meth. B, **97** (Proc. Suppl.), 231-234 (2001).
8. J. O. Gichaba, "Measurements of TYVEK Reflective Properties for the Pierre Auger Project," Ph.D. Thesis, The University of Mississippi (1998).
9. M. Janecek, W. W. Moses, "Simulating Scintillator Light Collection Using Measured Optical Reflectance," IEEE T. Nucl. Sci. **57**(3), 964-970 (2010).
10. J. C. Stover, "Optical scattering : measurement and analysis," SPIE Press (1995).
11. G. Hausler, "Limits of optical range sensors and how to exploit them," in *International Trends in Optics and Photonics ICO IV*, T. Asakura, ed., Springer Series in Optical Sciences (Springer Verlag, Berlin), **74**, 328342 (1999).
12. B. F. LeLoup, "Design of an instrument for measuring the spectral bidirectional scatter distribution function," Appl. Opt. **47**(3), 5454-5467 (2008).
13. Geant 4 User's Guide For Applications Developers, Geant4 Project homepage.

#135897 - $15.00 USD Received 30 Sep 2010; revised 7 Nov 2010; accepted 7 Dec 2010; published 17 Feb 2011

1. Introduction

Tyvek (DuPont registered trademark) is a popular material used in various applications for its durability and high reflectivity over a wide range in the UV/VIS region. For instance, it was selected for the inner lining of the Super-Kamiokande detector [1] and recently for the inner lining of water tanks at the Pierre Auger project [2] to increase the light collection efficiency of the Cherenkov light.

The Geant4 simulation toolkit is important and popular for the simulation of physics processes in various areas. In spite of its primary application in high-energy particle physics ([3, 4]) and astrophysics, it is also widely used for studies in space and medical science (popular GATE - Geant4 Application for Tomographic Emission [5]). The accuracy of Geant4 simulations depends on the credibility of both models of physics processes and the description of materials involved in simulations.

In the case of the Pierre Auger Observatory project, simulations of physics in surface detectors were performed for data processing and reconstructions in the Geant4 toolkit. This simulation is an example of incorporating detectors of Cherenkov light based on light collection by Tyvek. To have a complete model one needs to incorporate a model of the Tyvek reflection characteristics where diffusion plays a significant role.

Geant4 implements the UNIFIED model [6] for simulations of light scattering on diffuse and rough surfaces. One needs to measure the scatter profile of Tyvek to make up a reliable UNIFIED model of the Tyvek reflection characteristics. Diffuse characteristics and anisotropical effects of Tyvek were studied by Velazquez et al. [7]. The aim of their work was to measure the reflectivity of Tyvek in air and water but their results are not sufficient to set up a UNIFIED model. Some reflectivity tests were carried out by Gichaba in his Ph.D. thesis [8] which was directly devoted to surface detectors for the Pierre Auger Observatory project. In his thesis, he made up a model of surface detectors assuming that 70% of light scattered by Tyvek is due to Lambertian reflection and 30% is due to Gaussian reflection. There was not, however, any comparison between real data and the simulation.

The aim of this work is to measure accurately the scatter profile of Tyvek by means of measurements of the bidirectional reflectance distribution function (BRDF) and to calculate UNIFIED coefficients of Tyvek from these measurements. These coefficients are then incorporated into the Geant4 toolkit to setup a UNIFIED model of Tyvek reflection characteristics because this still has not been well implemented and insufficient approximations have been involved in the Geant4 simulations. As pointed out in [9], Tyvek has to be approximate as purely Lambertian reflector with present implementation of the UNIFIED model in Geant4 code. This issue is discussed in this work. In simulations, we needed to modify this implementation to get a reliable scatter profile with the UNIFIED model. The comparison between the real scatter profile and the simulated one was done to verify the updated model and to figure out its limitations.

Measurements of the BRDF were carried out with the CASI (by SMS co.) scatterometer, see Fig. 1. It measures the BRDF with an accuracy of 5%. Its arm length (sample-to-detector distance) is 575 mm. The beam spot diameter is $\approx$3 mm (the half-width of the Gauss profile of the spot). Our setup provides for measurements at 325 nm and 633 nm with the detector aperture 12.5 mm which is typical for measurements of diffuse samples . The angle increment is 0.415°. For surface anisotropy studies we combined scatter measurements with surface profile measurements acquired with the Talysurf Series 2 profilometer by Taylor-Hobson. It uses a 90° conical stylus with a spherical tip of 2 μm radius.

#135897 - $15.00 USD Received 30 Sep 2010; revised 7 Nov 2010; accepted 7 Dec 2010; published 17 Feb 2011

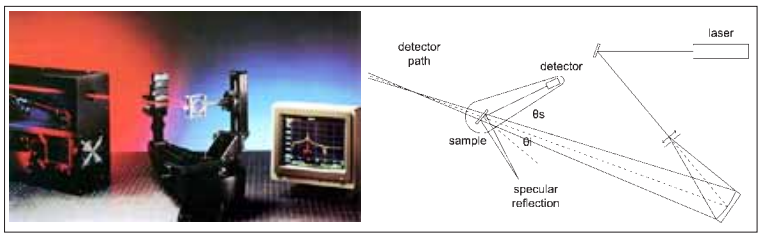

Fig. 1. The CASI scatterometer system.

2. Theoretical background

2.1. Bidirectional reflectance distribution function

The bidirectional reflectance distribution function (BRDF) f_s fully describes the reflection scatter profile of an optical sample. For a given sample, the BRDF is a function of the incidence angle, the angle of observation (or scatter) direction and the wavelength of light. The situation is sketched in Fig. 2. The $\vec{i}$ is the irradiance direction, $\vec{r}$ is the direction of specular reflection and $\vec{s}$ is the observation direction. If Φ_i is a light flux irradiating the sample of area dA then the BRDF is given by [10]:

$$f_s(\theta_i,\varphi_i;\theta_s,\varphi_s;\lambda) = \frac{\delta L(\theta_s,\varphi_s;\lambda)}{\delta E(\theta_i,\varphi_i;\lambda)} = \frac{d^2\Phi_s}{dA d\Omega_s \cos\theta_s}\frac{dA}{d\Phi_i} \cong \frac{d\Phi_s}{d\Omega_s}\frac{1}{\Phi_i\cos\theta_s}\ , \tag{1}$$

where δE is the irradiance of the sample facet of area dA, δL is the radiance contribution from the facet towards the observer (scatter direction) covering the solid angle $d\Omega_s$, and Φ_s is the scattered radiant flux.

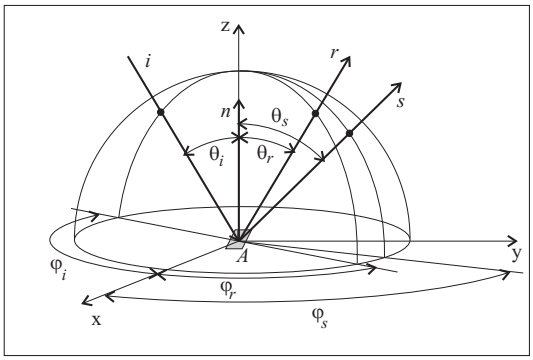

Fig. 2. Geometry for the definition of BRDF.

Let $J(\theta_i,\theta_s,\varphi_s) = d\Phi_s/d\Omega_s$ denote the radiant intensity of the scattered light. Then one can express the BRDF as a function of the radiant intensity:

$$f_{s,corr} \equiv f_s\cos\theta_s \cong \frac{1}{\Phi_i}J(\theta_i,\theta_s,\varphi_s)\ , \tag{2}$$

where $f_{s,corr}$ denotes the so-called cosine-corrected BRDF function.

#135897 - $15.00 USD Received 30 Sep 2010; revised 7 Nov 2010; accepted 7 Dec 2010; published 17 Feb 2011

2.2. UNIFIED model of rough surface scattering

The UNIFIED model was proposed by Levin and Moisan [6] to describe how to simulate scatter light on rough surfaces in Monte Carlo simulation toolkits. The UNIFIED model denotes the radiant intensity as a sum of four reflection components and one transmission component [6]:

$$\begin{aligned} J(\theta_i,\theta_s,\varphi_s) \quad \propto \quad & \Phi_i R(\theta_i)\left[C_{sl}\,g(\alpha_s,0,\sigma_\alpha)+C_{ss}\,\delta(\theta_i-\theta_s)\delta(\varphi_s)+C_{bs}\,\delta(\theta_i+\theta_i)\delta(\varphi_s)\right]+ \\ & +\Phi_i R(\theta_i)C_{dl}\cos\theta_s+\Phi_i T(\theta_t)g(\alpha_t,0,\sigma_\alpha)\ , \end{aligned} \tag{3}$$

where R denotes the surface reflectivity, T is the material transmittance, $g(\alpha,0,\sigma_\alpha)$ is a Gaussian distribution of angle deviations α of micro-facet normals with respect to the mean surface normal. Coefficients C_{sl}, C_{ss}, C_{bs}, and C_{dl} control the probability of specular lobe reflection around the normal of microfacets (C_{sl}), specular spike reflection around the average normal of the surface (C_{ss}), backward reflection (C_{bs}), and the Lambertian reflection (C_{dl}) [6] respectively.

The specular lobe reflection on microfacets is sketched in Fig. 3. The deviation of a microfacet normal $\vec{n}'_s$ from the mean surface normal $\vec{n}$ shifts the direction of the reflected light to the angle $\theta_s = 2\alpha_s + \theta_i$. Thus, we can express the Gaussian as a function of the scatter angle θ_s:

$$g(\alpha_s,0,\sigma_\alpha) = \exp\left[-\frac{\alpha_s^2}{2\sigma_\alpha^2}\right] = \exp\left[-\frac{(\theta_s-\theta_i)^2}{8\sigma_\alpha^2}\right]\ . \tag{4}$$

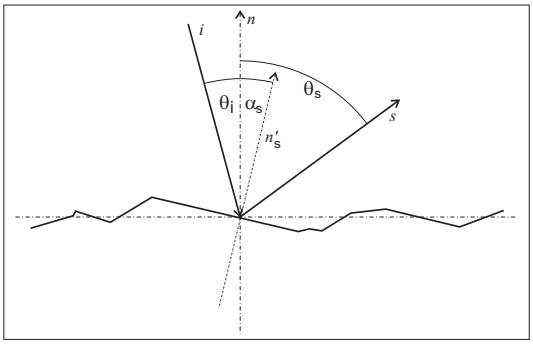

Fig. 3. Light reflection on a microfacet.

The light beam is reflected on a microfacet only if $\vec{i}\cdot\vec{n}'_s < 0$, otherwise the microfacet is hidden from a given incidence direction and its α_s is a blind angle (which corresponds to a not illuminated microfacet). Moreover the reflected light beam should satisfy $\vec{s}\cdot\vec{n} > 0$ to leave the surface. These two conditions cause the scattered light distribution to be dependent on the angle of incidence. The first condition causes the microfacet slope distribution to get narrower as seen from the increasing angle of incidence as well as causing it to loose its Gaussian distribution. Thus we get an 'effective' microfacet distribution of the surface with respect to the impacting light direction. As a result, the assumption of Gaussian distribution of microfacets slopes fails at higher angles. This shadowing effect causes, at high angles, the specular lobe reflection distribution to become narrower, asymptotically approaching a specular spike reflection distribution. This issue is discussed for instance in [9].

We take into account only the specular lobe and the Lambertian components to describe the scatter profile of Tyvek. The specular spike component is relevant for surfaces with RMS roughness less than $1/4$ of the light wavelength (polished surfaces) [11]. Otherwise, it is suppressed, as is the case of Tyvek. The backscatter spike component occurs when a light is reflected within

#135897 - $15.00 USD Received 30 Sep 2010; revised 7 Nov 2010; accepted 7 Dec 2010; published 17 Feb 2011

a deep groove on very rough surfaces but this is not the case of Tyvek. We do not assume any transmission component because we focused on the reflection profile. Thus the cosine-corrected BRDF function follows the relationship (by substitution of the Eq. (3) to the Eq. (2)):

$$f_{s,corr} \approx R(\theta_i)\left[C_{sl}\, g(\alpha_s, 0, \sigma_\alpha) + C_{dl}\cos\theta_s\right] . \tag{5}$$

2.3. Measurements of BRDF and probability of Gaussian and Lambertian reflection

In general, there are two possible approaches to acquire UNIFIED parameters from scatter measurements. The most general is to investigate the BRDF profile with a full 3D spatial coverage. Leloup et al. [12] gives a description of such an instrument.

For isotropic surfaces, it is also adequate to calculate UNIFIED parameters from in-plane BRDF profiles, which is our case. We calculated coefficients C_{sl} and C_{dl} by fitting an in-plane BRDF profile with Eq. (5). In this case, the correction to the entire reflection hemisphere is required. To do so, we need to estimate the contributions of both the specular lobe and the Lambertian components. Assuming the Eq. (2), the scattered light flux radiating in solid angle $d\Omega$ is equal to:

$$d\Phi_s = \Phi_i f_{s,corr} d\Omega_s = 2\pi\Phi_i f_{s,corr}\sin\theta_s d\theta_s . \tag{6}$$

We evaluated the following integrals to estimate the contributions of the specular lobe and the Lambertian components for an isotropic sample (integrating in the entire reflection hemisphere):

$$\begin{aligned}
\Phi_{s,dl} &= 2\pi\Phi_i R C_{dl}\int_0^{\pi/2}\cos\theta_s\sin\theta_s d\theta_s \equiv \Phi_i R k_1 C_{dl} , \\
\Phi_{s,sl} &= 2\pi\Phi_i R C_{sl}\int_0^{\pi/2}\exp\left[-\frac{(\theta_s-\theta_i)^2}{8\sigma_\alpha^2}\right]\sin(\theta_s-\theta_i)d(\theta_s-\theta_i) \equiv \Phi_i R k_2 C_{sl} ,
\end{aligned} \tag{7}$$

where $k_1 = 0.5$ and $k_2 = k_2(\theta_i, \sigma_\alpha)$ are evaluated by integration. Evaluation of the specular lobe contribution $\Phi_{s,sl}$ is valid for low θ_i as the specular lobe is significantly cut at higher angles of incidence (the condition $\vec{s}\cdot\vec{n} > 0$).

Now we can calculate the corrected coefficients $C_{sl,corr}$ and $C_{dl,corr}$ so that they express the probabilities of corresponding reflection components:

$$\begin{aligned}
C_{dl,corr} = \frac{\Phi_{s,dl}}{\Phi_{s,dl}+\Phi_{s,cl}} &= \frac{k_1 C_{dl}}{k_1 C_{dl} + k_2 C_{sl}} , \\
C_{sl,corr} = \frac{\Phi_{s,sl}}{\Phi_{s,dl}+\Phi_{s,cl}} &= \frac{k_2 C_{sl}}{k_1 C_{dl} + k_2 C_{sl}} ,
\end{aligned} \tag{8}$$

where the normalization due to the constrain $C_{sl,corr} + C_{dl,corr} = 1$ was applied. These corrected coefficients are proper for the Geant4 simulation toolkit.

3. Results

3.1. Surface anisotropy effects

First we measured the surface profile of the Tyvek 1025-BL sample to check the rate of its profile anisotropy by means of the Talysurf Series 2 profilometer. The evaluation length was selected in accordance with the standard recommended cut-off (ISO 4288-1996, EN ISO 4288:1997). The cut-off was 2.5 mm for non-periodic profiles and the evaluation length was 12.5 mm. The sampling spacing with the mentioned device was 0.250 μm. Measurements were done in the range of 0.167 mm in a vertical direction.

#135897 - $15.00 USD Received 30 Sep 2010; revised 7 Nov 2010; accepted 7 Dec 2010; published 17 Feb 2011

Let β denote the angle of the sample rotation around its surface normal and let $\beta = 0^\circ$ correspond to the sample rotational position equal to the position at which the main measurements over the angle of incidence were carried out (see section *Main measurements*). The sample was adjusted in four rotating directions $\beta = 0^\circ$, 45°, 90°, and -45° in order to inspect the surface anisotropy. Three sets of measurements were performed in each direction. Results are summarized in Table 1 in terms of profile roughness parameters.

Table 1. Surface profile parameters of Tyvek.

β [°]	R_a [μm]	R_q [μm]	R_t [μm]	R_z [μm]	R_{da} [rad]	R_{dq} [rad]
0	4.8 ± 0.5	6.0 ± 0.5	35.8 ± 4.3	30.0 ± 2.8	0.29 ± 0.01	0.39 ± 0.01
45	4.9 ± 0.5	6.2 ± 0.5	40.0 ± 4.9	31.7 ± 2.5	0.33 ± 0.01	0.43 ± 0.01
90	5.2 ± 0.5	6.6 ± 0.5	41.9 ± 2.1	34.7 ± 2.5	0.31 ± 0.01	0.40 ± 0.01
-45	4.8 ± 0.5	6.0 ± 0.5	37.5 ± 0.5	31.0 ± 1.5	0.29 ± 0.01	0.38 ± 0.01

The R_a is the arithmetic average roughness, R_q is the RMS roughness, R_t is the maximum height of the profile, R_z is the average distance between the highest peak and the lowest valley in each sampling length, R_{da} is the average absolute slope of the profile within the sampling length, and R_{dq} is the RMS slope of the profile within the sampling length of the surface.

The slope parameters R_{da} and R_{dq} and amplitude parameters R_a and R_q describe well the anisotropy of the surface profile. Comparing these parameters obtained at various β positions, we see the difference $\Delta R_{da} \approx 0.04$ rad, $\Delta R_{dq} \approx 0.04$ rad, $\Delta R_a \approx 0.4\ \mu m$, and $\Delta R_q \approx 0.6\ \mu m$. This means a slight anisotropy in the Tyvek surface profile.

Then the anisotropy effect was studied by scatter measurements. We performed several BRDF measurements on the scatterometer with the laser source at 633 nm to check how the scatter profile was influenced by the sample rotation position along its surface normal. We measured BRDF for angles of incidence $\theta_i = 0^\circ$ and $\theta_i = 60^\circ$. Following position angles β of the sample were investigated: 0°, 22°, 45°, 67°, and 90°. The results are plotted in Fig. 4. The cut near $\theta_s = -80^\circ$ is the shadow of the sample support intended for anisotropy measurements.

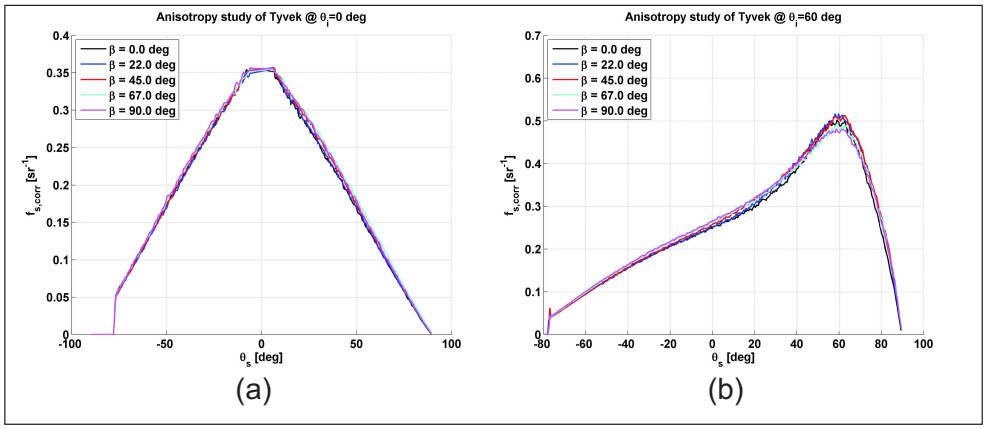

Fig. 4. Results of the surface anisotropy effect scans.

In the case of the $\theta_i = 0^\circ$ scan, the BRDF is cut on the top due to the detector shadow with a width of 8.02° (half-width 4.01°). For both incident angle scans, the mean relative deviation between each plotted BRDFs was 3% which is within the scatterometer accuracy of 5% for

#135897 - $15.00 USD Received 30 Sep 2010; revised 7 Nov 2010; accepted 7 Dec 2010; published 17 Feb 2011

BRDF measurements. Thus we can consider that the surface anisotropy effect is not significant.

3.2. Main measurements

We measured the BRDF function for incidence angles of 5°, 15°, 30°, 45°, 60°, and 75°. We skipped measurements at 0° due to the detector shadow in the scatter region where the Gaussian peak of the scattered light is located (see Fig. 4). This significant missing signal would distort a subsequent analysis. Instead, we started at 5°. We used two laser sources with 325 nm and 633 nm. The resulting BRDF functions are plotted in Fig. 5 for 325 nm with the corresponding fit results based on the Eq. (5). The RMSE error of fit is inserted into each graph to quantitatively estimate how well each fit corresponds to the data. The results with the 633 nm laser were similar and they are not plotted in the paper.

One can see that the assumptions for the reflection given by the combination of Lambertian and Gaussian terms (the Eq. (5)) are valid for angles up to 30° and they are acceptable at 45° (RMSE$<$0.01 sr^{-1}). For angles greater than 45°, a specular term comes into account and the fitting by means of the formula Eq. (5) deviates from the data. The reason is that the pure specular reflection becomes stronger with the increasing incidence angle at the expense of the Lambertian reflection.

Fitted UNIFIED parameters are summarized in Table 2. Parameters $C_{sl,corr}$ and $C_{dl,corr}$ are normalized by evaluation of the Eq. (8).

Table 2. Fitted normalized UNIFIED parameters.

θ_i [°]	$C_{dl,corr}$		$C_{sl,corr}$		σ_α [rad]	
	325 nm	633 nm	325 nm	633 nm	325 nm	633 nm
5	0.82 ± 0.05	0.83 ± 0.03	0.18 ± 0.05	0.17 ± 0.03	0.22 ± 0.02	0.22 ± 0.03
15	0.80 ± 0.03	0.78 ± 0.04	0.20 ± 0.03	0.22 ± 0.04	0.26 ± 0.02	0.27 ± 0.03
30	0.80 ± 0.02	0.80 ± 0.03	0.20 ± 0.02	0.20 ± 0.03	0.24 ± 0.02	0.24 ± 0.02
45	0.81 ± 0.02	0.79 ± 0.02	0.19 ± 0.02	0.21 ± 0.02	0.21 ± 0.02	0.20 ± 0.01
60	0.74 ± 0.02	0.73 ± 0.03	0.26 ± 0.02	0.27 ± 0.03	0.18 ± 0.02	0.17 ± 0.03
75	0.52 ± 0.04	0.57 ± 0.05	0.47 ± 0.04	0.43 ± 0.05	0.19 ± 0.02	0.15 ± 0.03

From Table 2, one can see that results are not dependent on the wavelength of the light source and the specular character of the reflection becomes more significant at higher incidence angles. We find mean corrected parameters $C_{sl,corr} = 0.20 \pm 0.04$ and $C_{dl,corr} = 0.80 \pm 0.04$ as a relevant approximation in applications where incidence angles up to 45° play the most significant role in the Geant4 simulation design. The parameter $\sigma_\alpha = 0.23 \pm 0.03$ rad in this incidence angle range is in agreement with the results by Gichaba [8] ($\sigma_\alpha = 0.19$ rad).

4. Implementation in Geant4

Geant4 implements the UNIFIED model [6] for simulations of light scattering on diffuse and rough surfaces. Until recently, its basic implementation had allowed for six types of surface finish [13]: polished (smooth, perfectly polished surface), polished front painted (top layer paint on polished surface), polished back painted (polished with back foil), ground (rough surface), ground front painted (top layer paint on rough surface) and ground back painted finish (rough back paint). The first three cases apply for the smooth surfaces with specular reflections. The ground finish type applies to transparent surfaces where the transmission and the reflection occur which are based on Fresnel equations and Snell's law. The ground front painted finish

#135897 - $15.00 USD Received 30 Sep 2010; revised 7 Nov 2010; accepted 7 Dec 2010; published 17 Feb 2011

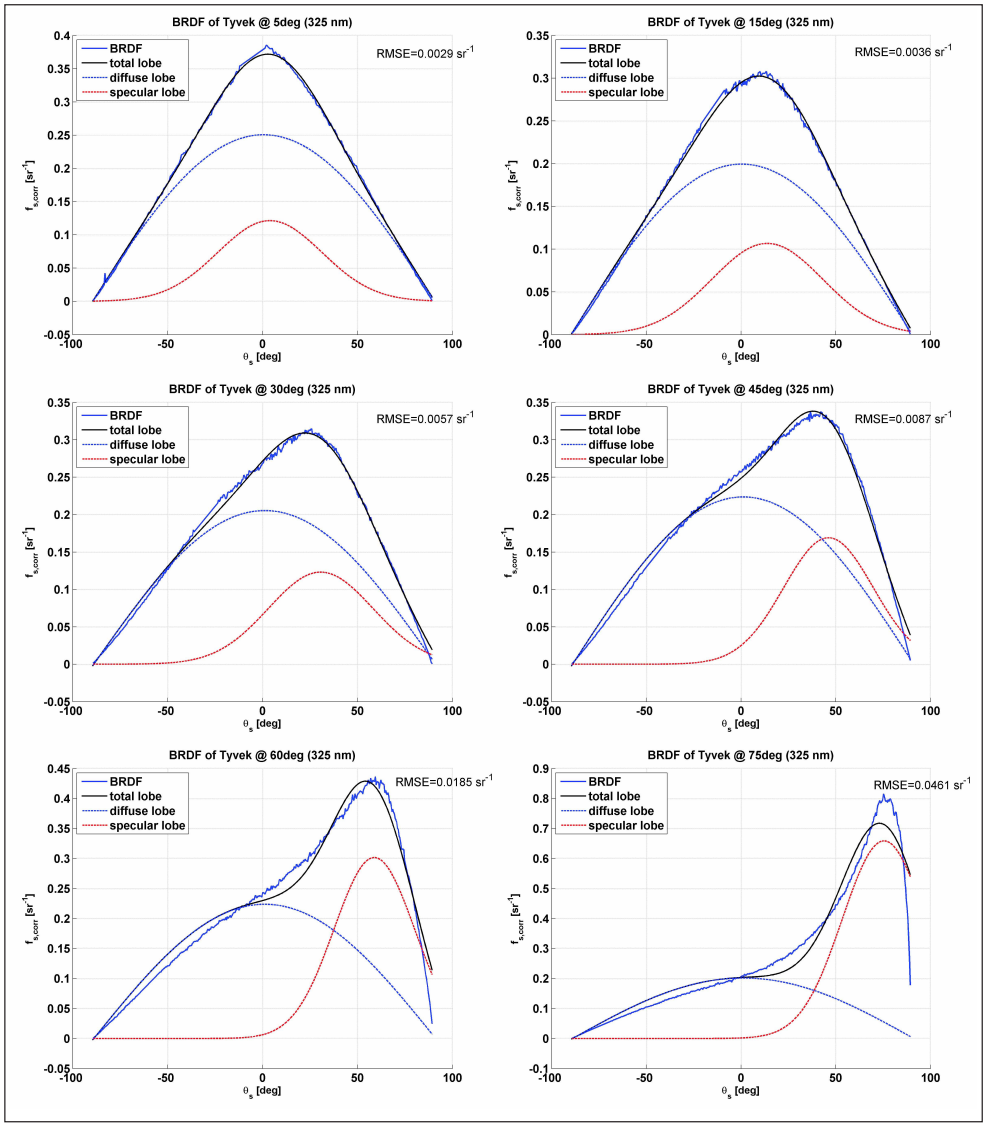

Fig. 5. BRDF functions of Tyvek for various angles of incidence.

is designed for materials with diffuse reflection (without transmission) with the Lambertian profile. The ground back painted finish is similar to the base ground surface in addition with the Lambertian reflection inside the material (transmission is suppressed).

Starting with version 9.3 of Geant4, finish types are extended by 24 new types of surfaces based on the work by Janecek and Moses [9] which in fact bypasses the UNIFIED model. New surface finish types are based on measuring the angular reflectivity distribution inside BGO (bismuth germanate) crystals with common surface treatments and reflectors applied. The light scatter is simulated by means of searching look-up-tables (LUT) with data based on measurements. The great advantage of this implementation is that it handles the scatter profile dependency on the incidence angle. This is an excellent way to model reliably the light collection from a scintillating crystal (up to now only BGO crystals) with its specific surface

#135897 - $15.00 USD Received 30 Sep 2010; revised 7 Nov 2010; accepted 7 Dec 2010; published 17 Feb 2011

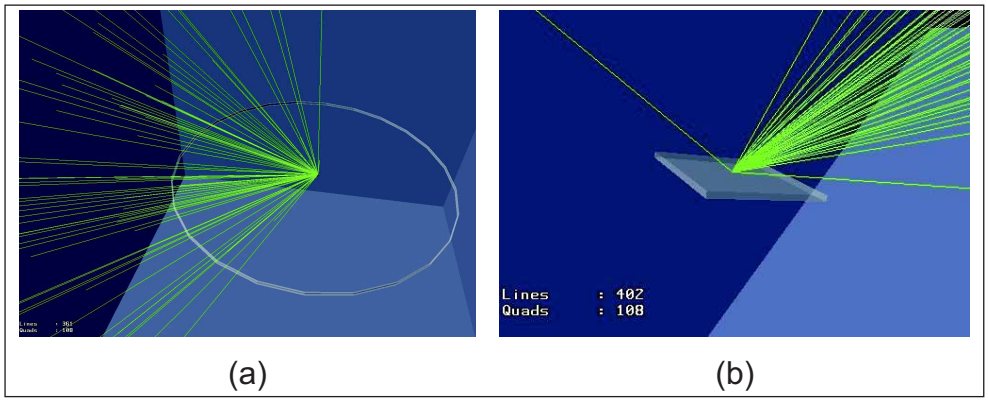

Fig. 6. (a) Simple CASI model, (b) sample detail.

treatment. An extension to other types of crystals will come in the future. Nevertheless, this LUT extension to the Geant4 toolkit is rather specific but it is not applicable in our case.

Choosing the UNIFIED model, the Geant4 toolkit uses coefficients C_{sl}, C_{ss}, C_{bs}, and C_{dl} to calculate a type of reflection within the frame of tracking the photon on the surface and inside the material so that the tracked photon generally undergoes additional Fresnel refractions while passing the surface from the material to the outside. As a result, the implementation of the model describes how to track a single photon on the surface rather than the requested global scatter profile of the reflected light. Thus, we extended the ground front painted type of the surface model by the specular lobe, the spike specular and the backscatter reflection.

Geant4 uses the reflectivity parameter R (see Eqs. (3) and (5)) to decide whether to absorb or to reflect a photon in the case of front painted and back painted materials. The reflectivity parameter is either provided by the user or calculated by means of Fresnel equations by Geant4. In the first case, only the specular dependency of reflectivity is accepted by Geant4 so that it is assumed constant over all angles of incidence. The latter case requires the knowledge of the complex index of refraction of material, which is problematic for Tyvek. Moreover in Geant4, the latter choice leads to the same problem with the manner of tracing a photon on the surface as discussed above and it is rather useful for a pure ground surface finish where transmission is included. That is why the first approach is recommended for Tyvek. We used the results of the Tyvek reflectivity measurements by Gichaba [8] and we set $R = 0.6$ at 325 nm and $R = 0.8$ at 633 nm.

We constructed a simple model of the CASI instrument (see Fig. 6) formed by a circle detector with the radius of 575 mm and a small movable Tyvek disk in the detector centre. We assigned the following material and optical properties to the sample: reflectivity $R = 0.6$ at 325 nm and $R = 0.8$ at 633 nm, standard deviation of the microfacet distribution $\sigma_\alpha = 0.23$ rad, specular lobe constant $C_{sl,corr} = 0.20$, and diffuse lobe constant $C_{dl,corr} = 0.80$. Comparisons between simulated output and real data in view of BRDF are illustrated in Fig. 7. Plots include the normalized root mean square deviation NRMSD. One can see that the model agrees with the measured data for incidence angles up to $\theta_i < 30^\circ$ with NRMSD<5%. The result NRMSD=5.5% for $\theta_i = 45^\circ$ is still acceptable.

5. Discussion

First we examined the surface anisotropy of the Tyvek sample. Results plotted in Fig. 4 show that its surface is isotropic within the frame of the accuracy of our BRDF measurements (the

#135897 - $15.00 USD Received 30 Sep 2010; revised 7 Nov 2010; accepted 7 Dec 2010; published 17 Feb 2011

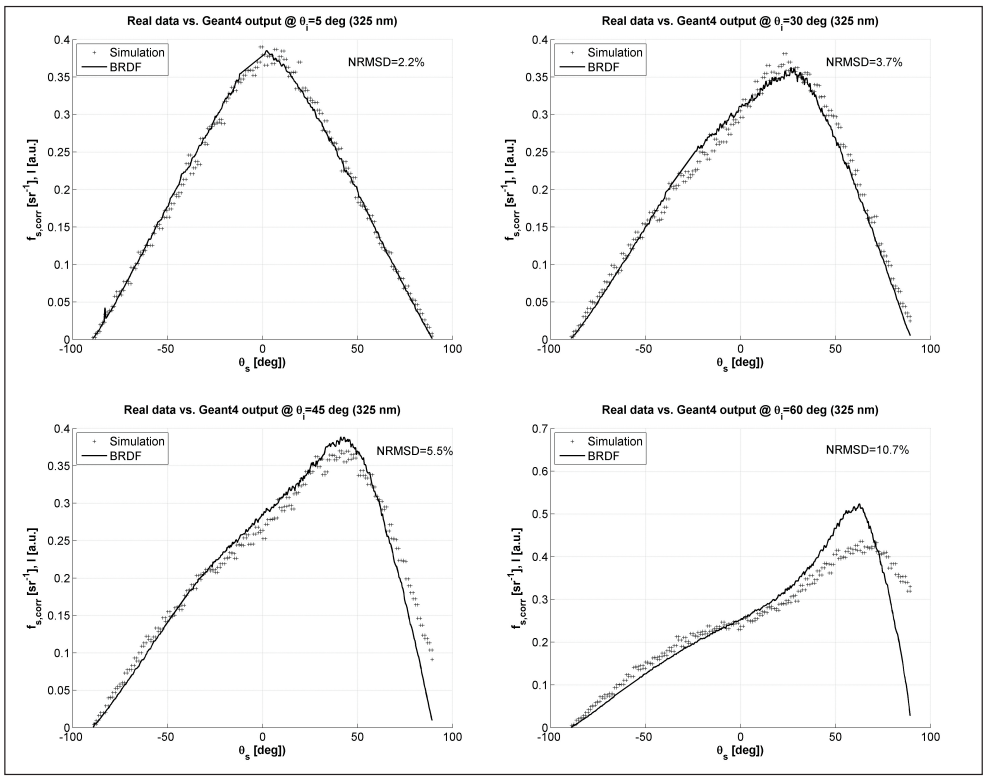

Fig. 7. Comparison between data and the Geant4 model.

scatterometer accuracy is 5%). The surface profilometry, see Table 1, gives us more precise results which indicate a slight surface profile anisotropy ($\Delta R_{da} \approx 0.04$ rad, $\Delta R_{dq} \approx 0.04$ rad, $\Delta R_a \approx 0.4\ \mu m$ and $\Delta R_q \approx 0.6\ \mu m$). However, the anisotropy is not evident in BRDF profiles because it is less than the uncertainty of the measurement.

As seen in Fig. 5, the BRDF function of the Tyvek material depends on the angle of incidence. The specular part of reflected light becomes narrower and amplified at high angles of incidence. Coefficients $C_{dl,corr}$ and $C_{sl,corr}$ given by the BRDF fitting at higher incidence angles (60° and greater) are rather orientational because corresponding fits are not sufficient. Moreover, the fitted σ_α coefficient gets significantly lower with the increasing incidence angle. The reason is that the effective surface profile significantly changes depending on the incidence direction and the pure specular reflection gains strength. The implementation of the UNIFIED model in the Geant4 toolkit takes into account only the first effect through the use of conditions $\vec{i} \cdot \vec{n}'_s < 0$ and $\vec{s} \cdot \vec{n} > 0$. The latter effect is not handled by Geant4 because UNIFIED parameters are constant over all angles of incidence. To measure these constants by light scatter methods, one should theoretically set the incidence angle to zero because only in this case does the σ_α coefficient correspond to the surface profile.

The validity of the results $C_{sl,corr} = 0.20$, $C_{dl,corr} = 0.80$ and $\sigma_\alpha = 0.23$ rad is constrained to incidence angles up to 45° also due to the estimation error of the specular lobe contribution $\Phi_{s,sl}$ given by the integral in the Eq. (7). This error grows with an increasing incidence angle.

The original UNIFIED implementation in the Geant4 does not generate outputs which correspond to our measured data. As said before, the model implementation describes how to track

#135897 - $15.00 USD Received 30 Sep 2010; revised 7 Nov 2010; accepted 7 Dec 2010; published 17 Feb 2011

single photons on the surface rather than a requested global scatter profile of the reflected light. One has to approximate the Tyvek material as a purely Lambertian reflector in original Geant4 code [9]. We have extended the ground front painted finish type of the surface model by the specular lobe, the spike specular, and the backscatter reflection to solve this problem. However, there is a model deviation from real data for angles 60° and greater.

One way to improve the light reflection model of diffuse materials in the Geant4 is to extend the UNIFIED implementation to be dependent on the angle of incidence, for example through the material properities tables with the specular spike coefficient nonzero at higher angles of incidence. The look-up-table approach is another way described in [9]. However, this needs a large amount of data gathered over a variety of materials.

6. Conclusion

We measured BRDF profiles of Tyvek, which is widely used in many applications. The main goal was to compute corresponding UNIFIED model parameters and incorporate them in Geant4 simulations. Corrections to the entire reflection hemisphere are necessary to estimate the probability of the Lambertian and the specular lobe reflection from in-plane BRDF measurements. We also needed to modify the UNIFIED model implementation in the Geant4 simulation toolkit to obtain the desired results in simulations. However, the model deviates at higher angles of incidence (greater than 45°). The drawback of the UNIFIED model is the lack of the possibility to setup its parameters as a function of the angle of incidence. Another solution is to use the look-up-tables design.

Acknowledgements

The authors gratefully acknowledge the support of the Operational Program Research and Development for Innovations - European Social Fund (project CZ.1.05/2.1.00/03.0058 of the Ministry of Education, Youth and Sports of the Czech Republic).

#135897 - $15.00 USD Received 30 Sep 2010; revised 7 Nov 2010; accepted 7 Dec 2010; published 17 Feb 2011